

Supplement of The Cryosphere, 12, 2545–2568, 2018  
<https://doi.org/10.5194/tc-12-2545-2018-supplement>  
© Author(s) 2018. This work is distributed under  
the Creative Commons Attribution 4.0 License.



*Supplement of*

## **The role of subtemperate slip in thermally driven ice stream margin migration**

**Marianne Haseloff et al.**

*Correspondence to:* Marianne Haseloff ([marianne.haseloff@earth.ox.ac.uk](mailto:marianne.haseloff@earth.ox.ac.uk))

The copyright of individual parts of the supplement might differ from the CC BY 4.0 License.

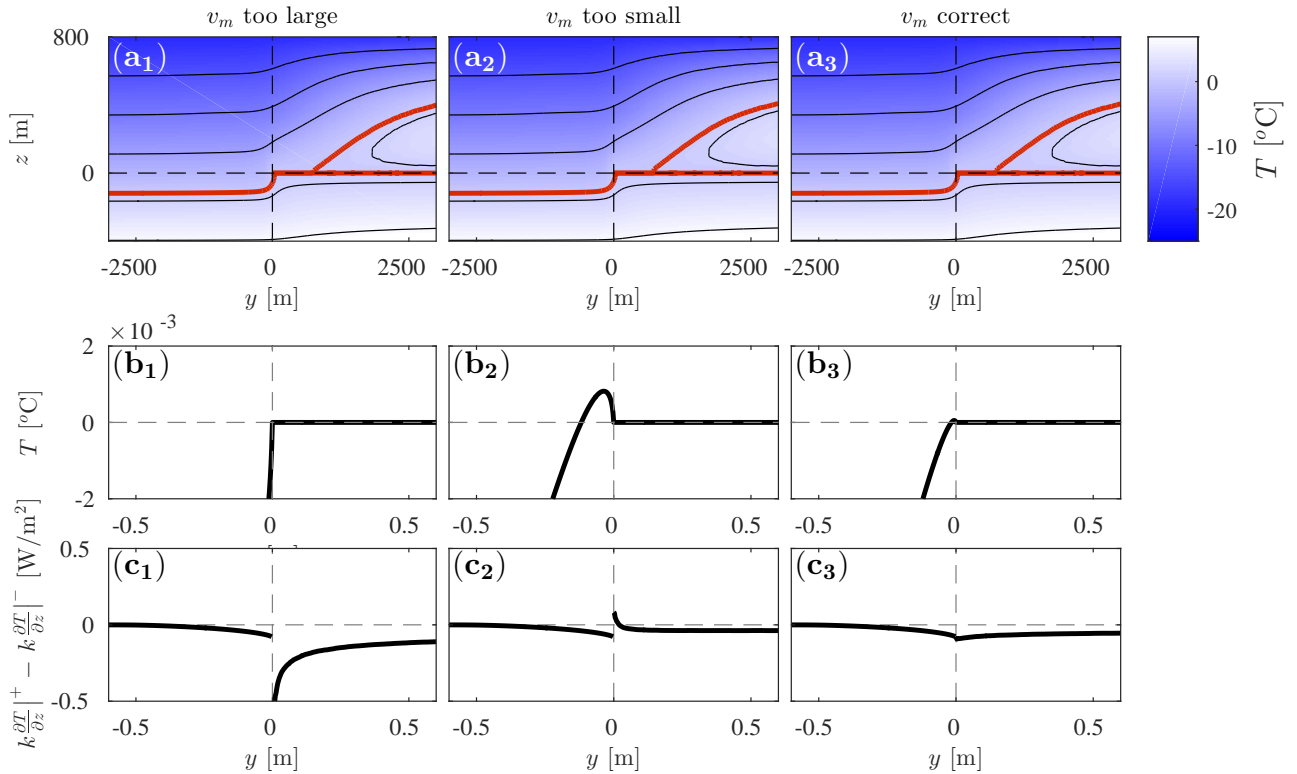


Figure S1: Numerical scheme to determine  $v_m$ . Each column (1-3) shows the temperature field (row a), temperature at the bed (row b) and net heat flux  $k(\partial T/\partial z|^+ - \partial T/\partial z|^-)$  into the bed (row c). Note that  $k(\partial T/\partial z|^+ - \partial T/\partial z|^-) = -\tau_c \sqrt{u^2 + v^2}$  for  $y < 0$ . Temperature contours are plotted in  $5^\circ\text{C}$  intervals, with  $T = 0^\circ\text{C}$  marked with a bold red line. Column 1 shows results for  $v_m = 0.70$  m/year and an apparently singular heat flux at the origin in panel c<sub>1</sub>. Column 2 shows results for  $v_m = 0.63$  m/year with constraint (17a)<sub>1</sub> violated in panel b<sub>2</sub>. Column 3 shows results for  $v_m = 0.65$  m/year, satisfying both constraints. Note that the results in rows b and c are plotted for a narrow range of  $y$  around the origin. The region in which the inequality constraints are violated can be quite small even for substantially incorrect values of  $v_m$ . This underlines the need for a high grid resolution around the origin in our computations. Calculations were done with  $h_s = 800$  m,  $q_r = 10^4$  m year<sup>-1</sup>,  $T_s = -20^\circ\text{C}$ ,  $A = 10^{-16}$ ,  $q_{\text{geo}} = 50$  mW m<sup>-2</sup>,  $\tau_s = 200$  kPa, and  $\tau_c = 5\tau_s = 1000$  kPa.

## 1 S1 Numerical scheme to determine the migration velocity

2 To illustrate how the migration rate is calculated, we show in figure S1 solutions to the heat flow  
3 problem without the inequality constraints (17a)–(17b) imposed. Figure S1 deliberately focuses on  
4 flow with subtemperate slip; for the case of a no-slip-to-free-slip transition, see figure 4.3 of Haseloff  
5 (2015) and figures 2 and 5 of Schoof (2012).

6 For ease of interpretation, we assume here (and in all other plots of the temperature field) that the  
7 melting point is at  $T_m = 0^\circ\text{C}$ . The three columns in the figure correspond to different migration rates  
8  $v_m = \partial y_m / \partial t$ . For each migration rate, the first row of panels (a<sub>1</sub>–a<sub>3</sub>) shows the resulting temperature  
9 field in the ice, the second row (b<sub>1</sub>–b<sub>3</sub>) shows the temperature  $T(y, 0)$  at the bed, and the third (c<sub>1</sub>–c<sub>3</sub>)  
10 shows  $k(\partial T/\partial z|^+ - \partial T/\partial z|^-)$ . On the cold side of the bed ( $y < 0$ ), this equals  $-\tau_c \sqrt{u^2 + v^2}$ . On the  
11 warm side of the bed, we require  $k(\partial T/\partial z|^+ - \partial T/\partial z|^-)$  to be finite.

12 In column 1, we show a calculation in which  $v_m$  is set to a value that is too large. This leads to  
13 a negative singular rate of melting for  $y > 0$  (panel c<sub>1</sub>), or in other words, a singular rate of freezing.  
14 By contrast, the middle (column 2) shows a case where  $v_m$  is too small. This results in temperatures  
15 exceeding the melting point in a small region on the supposedly frozen side of the transition ( $y < 0$ ,  
16 see panel b<sub>2</sub>). In column 3, we show results with a value of  $v_m$  for which the temperature is below the  
17 freezing point for  $y < 0$  and the freezing rate remains non-singular close to the origin. As discussed  
18 in appendix A and in the next section S2, this is the best we can hope for if we allow for slip with a

finite amount of basal friction  $\tau_c$  on the cold side of the transition: it is then not possible to suppress freezing completely.

In the present case, we cannot prove mathematically that there is a single migration rate for which neither inequality constraint in (17a)–(17b) is violated. Such a proof was however possible in the simpler version of our model in Schoof (2012), and computationally we find a unique  $v_m$  within bounds that are controlled by grid resolution. In practice, we determine the migration speed  $v_m$  iteratively using an adapted bisection method. The upper limit of the search interval is a migration velocity that is too large and therefore leads to a singular freezing rate on the ice stream side for  $y > 0$  which violates (17b)<sub>2</sub> (as in column 1 of figure S1). The lower limit of the search interval has temperatures at or above the melting point for  $y < 0$ , violating (17a)<sub>1</sub> (as in column 2 of figure S1). As with a standard bisection method, we halve the search interval at every iteration. We determine in which interval to continue the search based on which inequality constraint is violated at the midpoint: if (17a)<sub>1</sub> is violated we continue in the upper half, otherwise in the lower half (see also Haseloff et al., 2015).

## S2 Velocity, shear heating and temperature close to the cold-temperate transition

Here we extend the analysis of shear heating and temperature fields in appendix A of Schoof (2012) to the case of a transition from slip at a fixed basal yield stress  $\tau_c$  to free stress. Our purpose is to demonstrate mathematically that the temperature field near the origin (assumed to be the location at which the cold-temperate transition takes place) allows only the three different cases described above:

- 1) positive temperatures for  $y < 0$ , conflicting with the assumption that the bed there is subtemperate, and subtemperate sliding is taking place
- 2) an infinite heat flux out of the bed, corresponding to an infinite rate of basal freezing on the warm side of the origin  $y > 0$
- 3) as a limiting case, a finite rate of freezing on the warm side of the bed, equal to the dissipation rate on the subtemperate side of the bed

The numerical scheme in the previous section S1 is built on the assumption that the limiting case 3 is the only physically acceptable one.

For simplicity, we restrict ourselves to the case of constant ice viscosity  $\eta$ , and consider only flow parallel to the margin, assuming that the velocity component in the direction is much larger than the transverse velocity and therefore dominates the shear heating rate. We can treat the velocity as being the sum of a constant sliding velocity  $\bar{u}_b$  at the transition from frictional to free slip, and a correction  $\tilde{u}(y, z)$ . The latter then satisfies the Stokes flow problem

$$\eta \nabla^2 \tilde{u} = 0$$

for  $z > 0$ , where  $\nabla$  is the gradient operator in the transverse  $y$ - $z$ -plane, with boundary conditions

$$\eta \frac{\partial \tilde{u}}{\partial z} = \begin{cases} \tau_c & \text{at } z = 0, y < 0 \\ 0 & \text{at } z = 0, y > 0. \end{cases}$$

A general solution can be derived using complex variables, letting  $\zeta = y + iz$ , and using the differentiation rules (England, 1971)

$$\frac{\partial}{\partial y} = \frac{\partial}{\partial \zeta} + \frac{\partial}{\partial \bar{\zeta}} \quad \frac{\partial}{\partial z} = i \left( \frac{\partial}{\partial \zeta} - \frac{\partial}{\partial \bar{\zeta}} \right). \quad (\text{S1})$$

Since  $\tilde{u}$  satisfies Laplace's equation, it is the real part of a holomorphic function  $\phi(\zeta)$ ,  $\tilde{u}(y, z) = \text{Re}(\phi(\zeta))$ , and we have  $\partial \tilde{u} / \partial y + i \partial \tilde{u} / \partial z = \phi'(\zeta)$  (England, 1971). Continuing  $\phi'$  analytically to the lower half-plane  $\Im(\zeta) < 0$  by defining  $\phi'(\zeta) = \overline{\phi'(\bar{\zeta})}$  (note that  $\phi'$  has no physical meaning in the lower

58 half-plane), we find that the extended function  $\phi'$  is analytic in the  $\zeta$ -plane cut along the negative  
 59 half of the real axis, where it satisfies  $i(\phi'^+(y) - \phi'^-(y)) = 2\tau_c$ . The superscripts  $+$  and  $-$  indicate  
 60 limits taken from above and below, respectively. Hence an integrable solution takes the general form  
 61 (Muskhelishvili, 1992)

$$\phi'(\zeta) = -\frac{\tau_c}{\pi\eta} \log(\zeta) + \sum_{n=0}^{\infty} c_n \zeta^n,$$

62 where  $\log$  is the usual branch of the natural logarithm with a branch cut on the negative real axis, and  
 63 the  $c_n$  must be real to ensure the requisite symmetry of  $\phi'$ . The corresponding velocity field expressed  
 64 in polar coordinates, with  $y = r \cos(\vartheta)$  and  $z = r \sin(\vartheta)$ , is

$$\tilde{u} = \frac{\tau_c}{\pi\eta} \{r\vartheta \sin(\vartheta) - r[\log(r) - 1] \cos(\vartheta)\} + \sum_{n=0}^n \frac{c_n}{n+1} r^{n+1} \cos[(n+1)\vartheta].$$

65 Next, we consider the heat transport problem. At short enough length scales, several simplifications  
 66 can be made. To an error of  $O(\text{Per})$ , advection can be omitted, and the strain heating rate  $\eta|\nabla\tilde{u}|^2$  can  
 67 be approximated by retaining only the first two terms in the solution for  $\phi' \sim -\tau_c/(\pi\eta) \log(\zeta) + c_0$ . In  
 68 computing frictional dissipation due to sliding at the bed, we can also approximate the sliding velocity  
 69 by  $\tilde{u}_b$  to an error of  $O(r \log(r))$ . Hence, to an error of that magnitude,

$$-k\nabla^2 T = \begin{cases} \frac{\tau_c^2}{\pi^2\eta} [\log(r/r_0)^2 + \vartheta^2] & \text{for } z > 0, \\ 0 & \text{for } z < 0, \end{cases} \quad (\text{S2})$$

70 with the boundary conditions

$$T(y, 0) = 0 \quad \text{for } z = 0, y > 0, \quad (\text{S3})$$

$$-k \left[ \frac{\partial T}{\partial z} \right]_{-}^{+} = \tau_c \tilde{u}_b \quad \text{for } z = 0, y < 0, \quad (\text{S4})$$

$$[T(y, 0)]_{-}^{+} = 0 \quad \text{for } z = 0, y < 0 \quad (\text{S5})$$

71 where  $\log(r_0) = c_0\pi\eta/\tau_c$ . Importantly, the heat production rate for the no-slip to free-slip transition  
 72 in Schoof (2012) behaves as  $1/r$ , whereas it has only a logarithmic singularity in  $r$  here.

73 Using (S1), we can express Poisson's equation (S2) in terms of  $\zeta$  as

$$-4k \frac{\partial^2 T}{\partial \zeta \partial \bar{\zeta}} = \begin{cases} \frac{\tau_c^2}{\pi^2\eta} \log(\zeta/r_0) \log(\bar{\zeta}/r_0) & \text{for } \Im(\zeta) > 0 \\ 0 & \text{for } \Im(\zeta) < 0. \end{cases} \quad (\text{S6})$$

74 We can write the solution in the form

$$\begin{aligned} T = & -\frac{\tau_c^2}{8\pi^2 k \eta} \left\{ 2 [\zeta \log(\zeta/r_0) - \zeta] [\bar{\zeta} \log(\bar{\zeta}/r_0) - \bar{\zeta}] \right. \\ & - [\zeta \log(\zeta/r_0) - \zeta]^2 - [\bar{\zeta} \log(\bar{\zeta}/r_0) - \bar{\zeta}]^2 \\ & + 2i\pi [\zeta^2 \log(\zeta/r_0) - \bar{\zeta}^2 \log(\bar{\zeta}/r_0) + \bar{\zeta}^2 - \zeta^2] + i\pi (\zeta^2 - \bar{\zeta}^2) \left. \right\} \\ & + i \frac{\tau_c \tilde{u}_b}{2k} (\zeta - \bar{\zeta}) + \varphi(\zeta) + \overline{\varphi(\bar{\zeta})} \quad \text{for } \Im(\zeta) > 0 \\ T = & \varphi(\zeta) + \overline{\varphi(\bar{\zeta})} \quad \text{for } \Im(\zeta) < 0 \end{aligned}$$

75 where  $\varphi$  is an analytic function in the lower and upper half planes, its form to be determined by  
 76 the boundary conditions at the bed, where  $\Im(\zeta) = 0$ . Along the negative half of the real axis, the  
 77 boundary conditions (S4) and (S5) written in complex variable form using (S1) together ensure that  
 78  $\varphi'$  and therefore  $\varphi$  are continuous across that boundary and hence analytic on the  $\zeta$ -plane cut along  
 79 the positive real axis. On that branch cut,  $\varphi^+(y) + \overline{\varphi^+(y)} = \varphi^-(y) + \overline{\varphi^-(y)} = 0$ . Splitting  $\varphi$  into a  
 80 symmetric and antisymmetric part as  $\Omega(\zeta) = [\varphi(\zeta) + \overline{\varphi(\bar{\zeta})}]/2$  and  $\Psi(\zeta) = [\varphi(\zeta) - \overline{\varphi(\bar{\zeta})}]/2$ , it is then

81 straightforward to show that  $\Psi$  is analytic in the entire  $\zeta$  plane, while  $\Omega$  satisfies the homogeneous  
 82 Hilbert problem

$$\Omega^+(y) + \Omega^-(y) = 0$$

83 on the positive half of the real axis. Requiring an integrable heat flux  $\varphi'$ , we have a general solution

$$\varphi(\zeta) = \Omega(\zeta) + \Psi(\zeta) = -\zeta^{1/2} \sum_{n=0}^{\infty} \frac{ia_n}{2} \zeta^n - \sum_{n=0}^{\infty} \frac{ib_n}{2} \zeta^n$$

84 where  $\zeta^{1/2}$  has a branch cut on the positive half of the real axis, the limit taken from above being the  
 85 usual positive square root  $\sqrt{y}$ , and the  $a_n$  and  $b_n$  are purely real to satisfy the symmetries of  $\Omega$  and  
 86  $\Psi$ .

87 To an error of  $O(r^{5/2})$ , we therefore obtain a temperature field close to the origin of the form

$$\begin{aligned} T(r, \vartheta) = & \frac{\tau_c^2}{4\pi^2 k \eta} r^2 \left\{ \left[ \left( \log \left( \frac{r}{r_0} \right) - 1 \right)^2 + \vartheta^2 \right] - \cos(2\vartheta) \left[ \left( \log \left( \frac{r}{r_0} \right) - 1 \right)^2 - \vartheta^2 \right] \right. \\ & \left. + 2(\vartheta - \pi) \sin(2\vartheta) \left( \log \left( \frac{r}{r_0} \right) - 1 \right) - \pi \sin(2\vartheta) - 2\pi\vartheta \cos(2\vartheta) \right\} - \frac{\tau_c \bar{u}_b}{k} r \sin(\vartheta) \\ & + a_0 r^{1/2} \sin \left( \frac{\vartheta}{2} \right) + a_1 r^{3/2} \sin \left( \frac{3\vartheta}{2} \right) + b_1 r \sin(\vartheta) + b_2 r^2 \sin(2\vartheta) \end{aligned}$$

88 for  $0 < \vartheta < \pi$ , and

$$T(r, \vartheta) = a_0 r^{1/2} \sin \left( \frac{\vartheta}{2} \right) + a_1 r^{3/2} \sin \left( \frac{3\vartheta}{2} \right) + b_1 r \sin(\vartheta) + b_2 r^2 \sin(2\vartheta)$$

89 for  $\pi < \vartheta < 2\pi$ . The response to englacial shear heating is represented by the term in curly brackets,  
 90 which behaves as  $O(r^2 \log(r)^2)$ . The temperature is therefore dominated by the terms in the solution  
 91 to the problem without englacial heating, of the form

$$T \sim a_0 r^{1/2} \sin(\vartheta/2) + a_1 r^{3/2} \sin(3\vartheta/2) + b_1 r \sin(\vartheta) + b_2 r^2 \sin(2\vartheta) - \begin{cases} \frac{\tau_c \bar{u}_b}{k} r \sin(\vartheta) & \text{for } 0 < \vartheta < \pi \\ 0 & \text{otherwise.} \end{cases}$$

92 As in Schoof (2012), it is easy to see that we require  $a_0 \leq 0$  to ensure temperatures do not go above  
 93 freezing at the bed on the cold side of the transition point (that is, on  $\vartheta = \pi$ , where the leading order  
 94 form of  $T$  is then  $T \sim a_0 r^{1/2}$ ). A consequence of this is that, with  $a_0 \neq 0$ , we obtain a singular heat  
 95 flux  $-kr^{-1} \partial T / \partial \vartheta|_{\vartheta=0}^{\vartheta=2\pi} = ka_0 r^{-1/2}$  out of the bed on the warm side.

96 If we assume that a singular heat flux out of the bed is not viable as it leads to freezing of the  
 97 bed on the warm side of the transition, contradicting the assumption that the ice stream is widening,  
 98 then we must have  $a_0 = 0$ . The temperature field near the origin is then linear at leading order, and  
 99 can be written as  $T \sim b_1 z$  for  $z < 0$ ,  $T \sim [b_1 - \tau_c \bar{u}_b / k] z$  for  $z > 0$ , with the horizontal temperature  
 100 gradient only appearing at the next (higher) order.

101 There are two important conclusions that can be drawn from this. The first is that the net heat  
 102 flux out of the bed is

$$-\frac{1}{r} \frac{\partial T}{\partial \vartheta} \Big|_{2\pi}^0 = -\frac{1}{r} \frac{\partial T}{\partial \vartheta} \Big|_{\pi^+}^{\pi^-} = \tau_c \bar{u}$$

103 on both, the cold and the warm sides of the transition: it is impossible for the temperature gradient  
 104 to change discontinuously from the left to the right of the transition point. The fact that the frictional  
 105 heat  $\tau_c \bar{u}_b$  generated to the left of the transition must be removed from the bed means that heat is  
 106 removed at the same rate from the right, where presumably it must be supplied in the form of latent  
 107 heat transported by drainage of meltwater along the bed. The second observation is that it is no  
 108 longer necessary to have a region of temperate ice form near the transition point: if the temperature  
 109 below the bed is above the melting point, we expect  $b_1 < 0$  and hence  $\partial T / \partial z < 0$  everywhere above  
 110 the bed, corresponding to temperatures below the melting point in the ice.

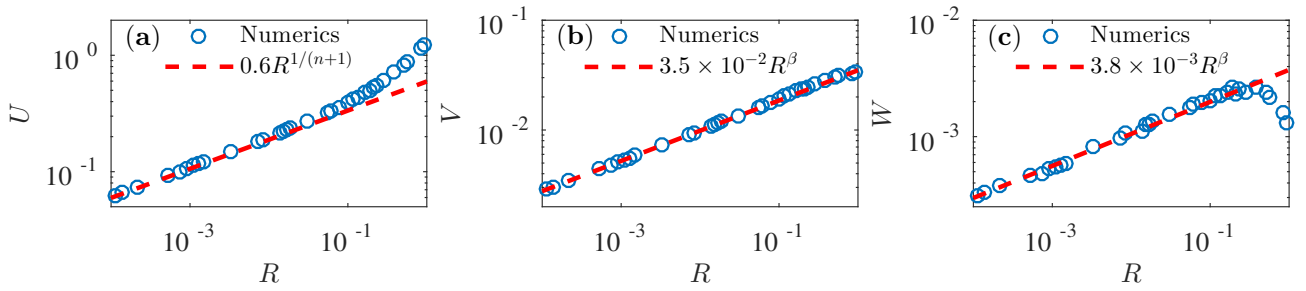


Figure S2: Comparison of numerical velocity solutions with asymptotic solutions from Rice (1967) and the solutions of the boundary value problem (S19)–(S21) for  $\vartheta = \pi/8$ . Panel a shows solutions of the downstream velocity  $U$ , panel b shows solutions of the across-stream velocity  $V$  and panel c shows solutions of the vertical velocity  $W$ .  $n = 3$  in all three cases.

### S3 The velocity field close to the transition from no slip to free slip

In section 4.3 we analyze the behavior of the temperature field close to the transition from no slip to free slip. To do so, we need to know the behavior of the velocities close to the origin, which we consider here. Near the origin of our geometry, i.e. for  $R = (Y^2 + Z^2)^{1/2} \rightarrow 0$  and for  $\varepsilon \ll 1$ , the equation for the down-stream velocity (22) with boundary conditions (29)–(30a) is identical to the model for a crack-tip considered in Rice (1967, 1968). He shows that in polar coordinates, the velocity solution close to the transition from free slip to no slip is of the form

$$U \sim C_u R^{\frac{1}{n+1}} \sqrt{\frac{2n}{n+1} A_\vartheta^{\frac{2}{n+1}} + \cos \vartheta A_\vartheta^{\frac{1-n}{1+n}}} \quad \text{for } R \rightarrow 0, \quad (\text{S7})$$

where  $R = \sqrt{Y^2 + Z^2}$ ,  $\cos \vartheta = Y/R$ ,  $C_u$  a constant that depends on the far field conditions, and

$$A_\vartheta = \frac{n^2 - 1}{4n} \cos \vartheta + \sqrt{\left(\frac{n^2 - 1}{4n}\right)^2 \cos^2 \vartheta + \frac{(n+1)^2}{4n}}. \quad (\text{S8})$$

Figures S2a and S3a confirm that our numerical solution reproduces this behavior as  $R \rightarrow 0$ . From (S7) the asymptotic behavior of the heat production rate (32) is

$$\mathcal{A} \sim \left(\frac{C_u}{2}\right)^{1+1/n} R^{-1} A_\vartheta^{-1}. \quad (\text{S9})$$

The important feature of this result is that the heat production is singular, behaving as  $R^{-1}$  near the transition point. This is not a surprise: a similar behavior for  $n = 1$  appears in Schoof (2004, 2012) and for  $n = 3$  in Suckale et al. (2014). For the frequently used special cases of  $n = 1$  and  $n = 3$ ,  $\mathcal{A}$  can alternatively be written as

$$\mathcal{A} \sim C_a R^{-1} \times \begin{cases} \text{const.} & \text{for } n = 1, \\ \left(\sqrt{3 + \cos^2 \vartheta} + \cos \vartheta\right)^{-1} & \text{for } n = 3. \end{cases} \quad (\text{S10})$$

The local behavior of the across-stream velocities ( $V, W$ ) is more difficult to determine. For a constant viscosity ( $n = 1$ ), Barcelona and MacAyeal (1993) show that

$$V \sim C_v R^{1/2} \left(2 \cos \frac{\vartheta}{2} + \sin \vartheta \sin \frac{\vartheta}{2}\right), \quad W \sim -C_w R^{1/2} \sin \frac{\vartheta}{2} \cos^2 \frac{\vartheta}{2}. \quad (\text{S11})$$

For  $n \neq 1$ , the problem of finding the local behavior of  $V$  and  $W$  is complicated by the fact that the viscosity is determined by  $|\nabla U|$ , where the local behavior of  $U$  is given by (S7). To find a generalization

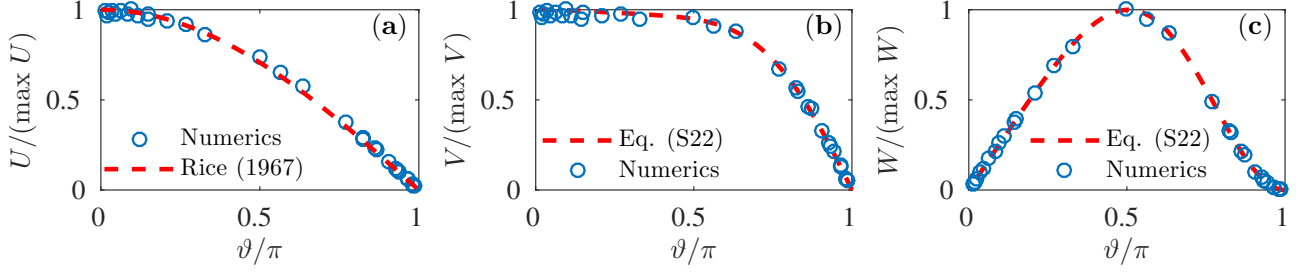


Figure S3: Comparison of numerical velocity solutions with asymptotic solutions from Rice (1967) and the solutions of the boundary value problem (S19)–(S21) for  $R = 0.01$ . Panel a shows scaled solutions of the downstream velocity  $U$ , panel b shows scaled solutions of the across-stream velocity  $V$  and panel c shows solutions of the vertical velocity  $W$ .  $n = 3$  in all three cases.

of (S11) for  $n \neq 1$ , we rewrite (23) in polar coordinates  $(R, \vartheta)$ :

$$-\frac{\partial P}{\partial R} + \frac{1}{R} \frac{\partial}{\partial R} (R \Sigma_{RR}) + \frac{1}{R} \frac{\partial \Sigma_{\vartheta R}}{\partial \vartheta} - \frac{\Sigma_{\vartheta \vartheta}}{R} = 0, \quad (\text{S12a})$$

$$-\frac{1}{R} \frac{\partial P}{\partial \vartheta} + \frac{1}{R^2} \frac{\partial}{\partial R} (R^2 \Sigma_{\vartheta R}) + \frac{1}{R} \frac{\partial \Sigma_{\vartheta \vartheta}}{\partial \vartheta} = 0, \quad (\text{S12b})$$

$$\frac{1}{R} \frac{\partial}{\partial R} (R V_R) + \frac{1}{R} \frac{\partial V_\vartheta}{\partial \vartheta} = 0. \quad (\text{S12c})$$

Here  $V_R$  and  $V_\vartheta$  are the radial and angular velocity components, respectively, i.e.,  $\mathbf{V} = V_R \mathbf{e}_R + V_\vartheta \mathbf{e}_\vartheta$ . The constitutive relations for the stresses  $\Sigma$  in polar coordinates are:

$$\Sigma_{RR} = \mu \frac{\partial V_R}{\partial R}, \quad \Sigma_{\vartheta \vartheta} = \mu \frac{1}{R} \left( \frac{\partial V_\vartheta}{\partial \vartheta} + V_R \right), \quad \Sigma_{\vartheta R} = \frac{1}{2} \mu \left( \frac{1}{R} \frac{\partial V_R}{\partial \vartheta} + \frac{\partial v_\vartheta}{\partial R} - \frac{v_\vartheta}{R} \right). \quad (\text{S13})$$

The boundary conditions (29) and (30a) at the base become

$$V_\vartheta = \mu \frac{1}{R} \frac{\partial V_R}{\partial \vartheta} = 0 \quad \text{for } \vartheta = 0, \quad V_\vartheta = V_R = 0 \quad \text{for } \vartheta = \pi. \quad (\text{S14})$$

The downstream velocity  $U$ , given by (S7)–(S8) determines the viscosity  $\mu$  through

$$\mu \sim R^{\frac{1-n}{1+n}} N \quad \text{with} \quad N(\vartheta) = [A_\vartheta(\vartheta)]^{\frac{n-1}{n+1}}. \quad (\text{S15})$$

We put  $\mu = R^{\frac{1-n}{1+n}} N$  and make the *ansatz*  $(V_R, V_\vartheta) = R^\beta (\bar{V}_R(\vartheta), \bar{V}_\vartheta(\vartheta))$  and  $P = R^{\beta-2/(n+1)} P_\vartheta(\vartheta)$ , which gives in (S12c)

$$\bar{V}_R + \frac{1}{\beta+1} \bar{V}_\vartheta' = 0. \quad (\text{S16})$$

Here a prime denotes an ordinary derivative with respect to  $\vartheta$ , so  $\bar{V}_\vartheta' = d\bar{V}_\vartheta/d\vartheta$ . Equations (S12a)–(S12b) become

$$-a_0 P_\vartheta - a_1 N \bar{V}_\vartheta' + (a_2 N \bar{V}_\vartheta - a_3 N \bar{V}_\vartheta'')' = 0, \quad (\text{S17a})$$

$$-P_\vartheta' + b_1 N \bar{V}_\vartheta - b_2 N \bar{V}_\vartheta'' + b_3 (N' \bar{V}_\vartheta' + N \bar{V}_\vartheta'') = 0, \quad (\text{S17b})$$

where

$$a_0 = \left[ \beta - \frac{2}{n+1} \right], \quad a_1 = \frac{\beta}{\beta+1} \left[ \beta + \frac{2n}{n+1} \right], \quad a_2 = \frac{(\beta-1)}{2}, \quad a_3 = \frac{1}{2} \frac{1}{\beta+1},$$

$$b_1 = \frac{1}{2} \left( \beta + \frac{2n}{n+1} \right) (\beta-1), \quad b_2 = \frac{1}{2} \left( \beta + \frac{2n}{n+1} \right) \frac{1}{\beta+1}, \quad b_3 = \frac{\beta}{\beta+1}.$$

137

138 Elimination of the pressure in (S17a) by use of (S17b) leads to a fourth order homogeneous differ-  
 139 ential equation for  $\bar{V}_\vartheta$  with non-constant coefficients

$$0 = \left(b_1 + c_5 \frac{N''}{N}\right) \bar{V}_\vartheta + \left(c_4 \frac{N'}{N} - c_2\right) V'_\vartheta + \left(c_3 - \frac{N''}{N}\right) \bar{V}_\vartheta'' - 2 \frac{N'}{N} \bar{V}_\vartheta''' - \bar{V}_\vartheta'''' \quad (\text{S19})$$

140 where

$$c_1 = \frac{a_0}{a_3} b_1, \quad c_2 = \frac{a_1}{a_3}, \quad c_3 = \frac{a_0}{a_3} (b_2 - b_3) + \frac{a_2}{a_3}, \quad c_4 = \left[2 \frac{a_2}{a_3} - \frac{a_1}{a_3} - \frac{a_0}{a_3} b_3\right], \quad c_5 = \frac{a_2}{a_3}, \quad (\text{S20})$$

141 and  $N$  is given by equation (S15). The boundary conditions (S14) are likewise homogeneous,

$$\bar{V}_\vartheta = \bar{V}_\vartheta'' = 0 \quad \text{for } \vartheta = 0, \quad \bar{V}_\vartheta = \bar{V}_\vartheta' = 0 \quad \text{for } \vartheta = \pi, \quad (\text{S21})$$

142 and we have a generalized eigenvalue problem in which the eigenvalue  $\beta$  is somewhat unconventionally  
 143 hidden in the coefficients (S20). We solve this problem using a shooting method, which gives  $\beta =$   
 144  $0.271\dots$  as the lowest positive eigenvalue for  $n = 3$ . Once again we find that our numerical solutions  
 145 reproduce this behavior, see figure S2b-c. Note that  $\beta$  is greater than  $1/(1+n)$ , so that the viscosity  
 146 is indeed dominated by gradients of the downstream velocity  $U$ . The shooting method also gives us  
 147  $V_\vartheta$ , from which  $V_R$  can be calculated through equation (S16). The velocity components  $(V, W)$  in  
 148 Cartesian coordinates can be calculated from  $(\bar{V}_R, \bar{V}_\vartheta)$  through

$$V = R^\beta (\bar{V}_R \cos \vartheta - \bar{V}_\vartheta \sin \vartheta), \quad W = R^\beta (\bar{V}_R \sin \vartheta + \bar{V}_\vartheta \cos \vartheta). \quad (\text{S22})$$

149 The angular dependence of  $U$ ,  $V$  and  $W$  is shown in figure S3.

150 Note that the local solution we have derived here stems from a problem (equations (22)–(30b) of  
 151 the main text) that contains no free parameters when — as we have assumed here —  $\tau$  is infinite. As  
 152 a result, we are guaranteed that  $C_a$ ,  $C_u$ ,  $\bar{V}_R$  and  $\bar{V}_\vartheta$  are also parameter-free, as is implied in the main  
 153 text.

## 154 S4 The outer temperature problem for strong heat production

155 In the main text, the velocity field derived in section S3 above is used to construct a local advection-  
 156 diffusion problem for heat transport near the cold-temperate (and no-slip-to-slip) transition. That  
 157 local model, equations (40) of the main text, is mathematically a boundary layer. It only depends on  
 158  $\Lambda$  and  $\tilde{V}_m$  as parameters, suggesting that  $\tilde{V}_m = \tilde{f}(\Lambda)$ , if the far-field conditions on the boundary layer  
 159 only depend on  $\Lambda$ , too. These boundary conditions mathematically come out of asymptotic matching  
 160 with an ‘outer’ problem that describes heat transport at a larger scale (Holmes, 2013). Here we verify  
 161 that matching leads to far-field conditions that only depend on  $\Lambda$  as required.

162 The outer problem to the conductive boundary layer itself describes heat flow in a slender region  
 163 along the bed. To identify leading order terms in this outer problem (confusingly, itself a boundary  
 164 layer to the advection-dominated heat transport across the bulk of the ice thickness), we first need  
 165 to understand the transverse velocity field near the bed.  $V = 0$  implies that  $\partial V / \partial Y = 0$  at the  
 166 bed, so  $\partial W / \partial Z = 0$  by mass conservation. By Taylor expansion, we obtain  $V \sim Z$ ,  $W \sim Z^2$ .  
 167 Near-bed advection in the outer problem is captured by considering a thin region of vertical extent  
 168  $Z_{\text{Pe}} = \text{Pe}^{-\beta/(1+\beta)} \ll 1$  relative to ice thickness, labeled the ‘advective boundary layer’ in figure 5.  
 169 Within this region, we rescale  $Z = Z_{\text{Pe}} \hat{Z}$ ,  $V = Z_{\text{Pe}} \hat{V}$ ,  $W = Z_{\text{Pe}}^2 \hat{W}$ ,  $\mathcal{A} = \hat{\mathcal{A}}$ ,  $\Theta = \hat{\Theta}$ .

170 Note that the vertical coordinate in the advective region is related to the vertical coordinate in  
 171 the conductive boundary layer through  $\hat{Z} = \Lambda^{-1} \text{Pe}^{(1-\beta)/(1+\beta)} \tilde{Z}$ . For  $\beta < 1$ ,  $\hat{Z} = O(1)$  implies that  
 172  $\tilde{Z} \gg 1$ . For  $n = 1$ , the exponent  $\beta$  equals  $1/2$ , and for  $n = 3$  we have  $\beta \approx 0.27$  (see supplementary  
 173 section S3). Therefore the near-bed advective layer is a viable outer region to the conductive boundary  
 174 layer because the advective layer has a much larger vertical and horizontal extent than the conductive  
 175 boundary layer.



176 For  $n = 3$  (or generally for  $n > 1$  and  $\beta < 1/2$ ), the outer problem is,

$$\tilde{V}_m \frac{\partial \hat{\Theta}}{\partial \hat{Y}} + \Lambda \left( \hat{V} \frac{\partial \hat{\Theta}}{\partial \hat{Y}} + \hat{W} \frac{\partial \hat{\Theta}}{\partial \hat{Z}} \right) = a \quad \text{for } 0 < \hat{Z}, \quad (\text{S23a})$$

$$\tilde{V}_m \frac{\partial \hat{\Theta}}{\partial \hat{Y}} = 0 \quad \text{for } \hat{Z} < 0, \quad (\text{S23b})$$

177 to an error of  $O(\text{Pe}^{(2\beta-1)/(1+\beta)})$ . As required, (S23a)–(S23b) only depend on  $\tilde{V}_m$  and  $\Lambda$ . As we are  
 178 considering an outer problem that describes a slender region near the bed, our choice of reduced  
 179 temperature  $\Theta$  means that the relevant boundary condition is  $\hat{\Theta}(\hat{Z} = 0) \rightarrow 0$  as  $Y \rightarrow -\infty$ , equation  
 180 (34c), which equally does not depend on any additional parameters.

## 181 S5 Mechanical problem for a small slip region: $\tau \sim \alpha^{1/(n+1)} \gg 1$

182 When we allow for subtemperate sliding, but at a large basal yield stress  $\tau \gg 1$ , the velocity field will  
 183 change only by a small amount: over most of the domain, basal shear stress will not attain the yield  
 184 stress. The only location where that is not the case is close to the origin, where a hard transition from  
 185 slip to no slip would lead to a stress singularity, exceeding any finite yield stress. In other words, the  
 186 region of slip created by a large but finite  $\tau$  is a mechanical boundary layer close to the origin, which  
 187 remains small compared with the ice thickness. Outside that boundary layer, the velocity field will  
 188 remain unchanged. In fact, at length scales that are intermediate between the boundary layer and the  
 189 ice thickness scales, the local solution of supplementary section S4 will still apply, and provides the  
 190 appropriate matching conditions on the mechanical boundary layer created by the small slip region.  
 191 In this section, we construct a leading order model for that boundary layer. We focus on the case  
 192 of  $\tau \sim \alpha^{1/(n+1)} \gg 1$ , in which the size of this mechanical boundary layer is the same as the size of  
 193 the thermal boundary layer: this is the minimum size of the mechanical boundary layer at which we  
 194 expect to start seeing an effect of subtemperate sliding on margin migration.

195 We rescale the mechanical field equations using  $(Y, Z) = R_\alpha(\tilde{Y}, \tilde{Z})$ ,  $\mathcal{A} = R_\alpha^{-1}\tilde{\mathcal{A}}$ ,  $U = R_\alpha^{1/(n+1)}\tilde{U}$ ,  
 196  $(V, W) = R_\alpha^\beta(\tilde{V}, \tilde{W})$ , and  $P = R_\alpha^{-1/(n+1)}\tilde{P}$  where  $R_\alpha = \alpha^{-1}$ . The choice of exponent  $\beta$  ensures that  
 197 the boundary layer solution can be matched with the outer problem at the ice thickness scale, whose  
 198 behavior in the matching region (Holmes, 2013) is given by supplementary section S4 as discussed.  
 199 This yields an equation for the velocity in the downstream direction of the same form as (22):

$$\frac{\partial}{\partial \tilde{Y}} \left( \tilde{\mu} \frac{\partial \tilde{U}}{\partial \tilde{Y}} \right) + \frac{\partial}{\partial \tilde{Z}} \left( \tilde{\mu} \frac{\partial \tilde{U}}{\partial \tilde{Z}} \right) = 0. \quad (\text{S24})$$

200 In the across-stream direction, we obtain from (23)

$$\frac{\partial}{\partial \tilde{Y}} \left( 2\tilde{\mu} \frac{\partial \tilde{V}}{\partial \tilde{Y}} \right) + \frac{\partial}{\partial \tilde{Z}} \left[ \tilde{\mu} \left( \frac{\partial \tilde{V}}{\partial \tilde{Z}} + \frac{\partial \tilde{W}}{\partial \tilde{Y}} \right) \right] - \frac{\partial \tilde{P}}{\partial \tilde{Y}} = 0, \quad (\text{S25a})$$

$$\frac{\partial}{\partial \tilde{Y}} \left[ \tilde{\mu} \left( \frac{\partial \tilde{V}}{\partial \tilde{Z}} + \frac{\partial \tilde{W}}{\partial \tilde{Y}} \right) \right] + \frac{\partial}{\partial \tilde{Z}} \left( 2\tilde{\mu} \frac{\partial \tilde{W}}{\partial \tilde{Z}} \right) - \frac{\partial \tilde{P}}{\partial \tilde{Z}} = 0, \quad (\text{S25b})$$

$$\frac{\partial \tilde{V}}{\partial \tilde{Y}} + \frac{\partial \tilde{W}}{\partial \tilde{Z}} = 0. \quad (\text{S25c})$$

201  $\mu$  is the rescaled non-dimensional viscosity

$$\tilde{\mu} = \frac{1}{2^{1/n}} \left[ \left| \frac{\partial \tilde{U}}{\partial \tilde{Y}} \right|^2 + \left| \frac{\partial \tilde{U}}{\partial \tilde{Z}} \right|^2 \right]^{\frac{1-n}{2n}}. \quad (\text{S26})$$

202 As before, we find for the vertical velocity component along the bed

$$\tilde{W} = 0 \quad \text{at} \quad \tilde{Z} = 0. \quad (\text{S27})$$

203 Similarly, the free slip boundary condition (29) on the temperate side remains unchanged

$$\tilde{\mu} \frac{\partial \tilde{U}}{\partial \tilde{Z}} = \tilde{\mu} \frac{\partial \tilde{V}}{\partial \tilde{Z}} = 0 \quad \text{at } \tilde{Z} = 0, \quad \tilde{Y} > 0. \quad (\text{S28})$$

204 On the frozen side of the bed, we have from (30b)

$$\left. \begin{array}{l} \text{either } \tilde{\mu} \frac{\partial \tilde{U}}{\partial \tilde{Z}} = \alpha^{1/(n+1)} \tau \frac{\tilde{U}}{|\tilde{U}|}, \quad \tilde{\mu} \frac{\partial \tilde{V}}{\partial \tilde{Z}} = \alpha^{1/(n+1)} \tau \frac{\tilde{V}}{|\tilde{U}|}, \quad |\tilde{U}| > 0, \quad |\tilde{V}| > 0 \\ \text{or } \left| \tilde{\mu} \frac{\partial \tilde{U}}{\partial \tilde{Z}} \right| < \alpha^{1/(n+1)} \tau, \quad \left| \tilde{\mu} \frac{\partial \tilde{V}}{\partial \tilde{Z}} \right| < \alpha^{1/(n+1)} \tau \left| \frac{\tilde{V}}{\tilde{U}} \right|, \quad |\tilde{U}| = |\tilde{V}| = 0 \end{array} \right\} \text{for } \tilde{Y} < 0, \quad \tilde{Z} = 0. \quad (\text{S29})$$

205 Equations (S24)–(S29) only depend on  $\alpha^{1/(n+1)} \tau = \Gamma^{-(n+1)}$ , as required for (46) to hold.

## 206 S6 Limit of large slip region: $\tau_c \ll \tau_s$

207 We conclude by considering the opposite parametric limit in  $\tau$  to that considered above: we derive  
 208 an otherwise elusive closed-form expression for  $V_m$  in the limit  $\tau \ll 1$ . When considering the case of  
 209 small basal yield stress  $\tau$ , the region of subtemperate slip becomes wide compared with ice thickness.  
 210 Simultaneously, we consider the case of  $\alpha \gg 1$ ,  $\text{Pe} \gg 1$ , identifying the relevant distinguished limit as  
 211  $\tau \text{Pe} \sim \alpha^2 \gg 1$  later.

212 There are two rescalings required: first, for the mechanical problem and second, for the thermal  
 213 problem. For the mechanical problem, we put

$$\hat{Y} = \tau Y, \quad \hat{Z} = Z, \quad \hat{U} = \tau U, \quad \hat{V} = V, \quad \hat{W} = \tau^{-1} W, \quad \hat{P} = \tau^{-1} P. \quad (\text{S30})$$

214 Under this rescaling, the mechanical problem in the boundary layer becomes

$$\tau^2 \frac{\partial}{\partial \hat{Y}} \left( \hat{\mu} \frac{\partial \hat{U}}{\partial \hat{Y}} \right) + \frac{\partial}{\partial \hat{Z}} \left( \hat{\mu} \frac{\partial \hat{U}}{\partial \hat{Z}} \right) = 0, \quad (\text{S31a})$$

$$\tau^2 \frac{\partial}{\partial \hat{Y}} \left( 2\hat{\mu} \frac{\partial \hat{V}}{\partial \hat{Y}} \right) + \frac{\partial}{\partial \hat{Z}} \left[ \hat{\mu} \left( \frac{\partial \hat{V}}{\partial \hat{Z}} + \tau^2 \frac{\partial \hat{W}}{\partial \hat{Y}} \right) \right] - \tau^2 \frac{\partial \hat{P}}{\partial \hat{Y}} = 0, \quad (\text{S31b})$$

$$\frac{\partial}{\partial \hat{Y}} \left[ \hat{\mu} \left( \frac{\partial \hat{V}}{\partial \hat{Z}} + \tau^2 \frac{\partial \hat{W}}{\partial \hat{Y}} \right) \right] + \frac{\partial}{\partial \hat{Z}} \left( 2\hat{\mu} \frac{\partial \hat{W}}{\partial \hat{Z}} \right) - \frac{\partial \hat{P}}{\partial \hat{Z}} = 0, \quad (\text{S31c})$$

$$\frac{\partial \hat{V}}{\partial \hat{Y}} + \frac{\partial \hat{W}}{\partial \hat{Z}} = 0, \quad (\text{S31d})$$

215 where

$$\hat{\mu} = \frac{1}{2^{1/n}} \left[ \left( \frac{\partial \hat{U}}{\partial \hat{Y}} \right)^2 + \tau^{-2} \left( \frac{\partial \hat{U}}{\partial \hat{Z}} \right)^2 \right]^{(1-n)/(2n)} \quad (\text{S32})$$

216 for  $0 < \hat{Z} < 1$ . Assume that there is slip for  $\hat{Y}_0 < \hat{Y} < 0$ , meaning  $\hat{U} > 0$  at  $\hat{Z} = 0$ . In that region, we  
 217 then have the following boundary conditions

$$\hat{\mu} \frac{\partial \hat{U}}{\partial \hat{Z}} = 0, \quad \hat{\mu} \left( \frac{\partial \hat{V}}{\partial \hat{Z}} + \tau^2 \frac{\partial \hat{W}}{\partial \hat{Y}} \right) = 0, \quad \hat{W} = 0 \quad \text{for } \hat{Y} > 0, \quad \hat{Z} = 0, \quad (\text{S33a})$$

$$\hat{\mu} \frac{\partial \hat{U}}{\partial \hat{Z}} = \tau^2, \quad \hat{\mu} \left( \frac{\partial \hat{V}}{\partial \hat{Z}} + \tau^2 \frac{\partial \hat{W}}{\partial \hat{Y}} \right) = \tau^2 \frac{\hat{V}}{\hat{U}}, \quad \hat{W} = 0 \quad \text{for } \hat{Y}_0 < \hat{Y} < 0, \quad \hat{Z} = 0. \quad (\text{S33b})$$

218 Expanding as  $\hat{U} = \hat{U}^{(0)} + \tau^2 \hat{U}^{(1)} + \dots$ ,  $\hat{V} = \hat{V}^{(0)} + \tau^2 \hat{V}^{(1)} + \dots$ ,  $\hat{W} = \hat{W}^{(0)} + \tau^2 \hat{W}^{(1)} + \dots$ , we find  
 219 that  $\hat{U}^{(0)} = \hat{U}^{(0)}(\hat{Y})$ ,  $\hat{V}^{(0)} = \text{constant}$ ,  $\hat{W}^{(0)} = 0$ . In other words, a wide region of subtemperate slip  
 220 implies that the plug flow of the ice stream extends past the thermal margin of the ice stream into a

221 rapidly sliding but cold-based region. The axial velocity  $\widehat{U}^{(0)}$  here satisfies the ice-stream-like model  
 222 for a laterally sheared plug flow with constant basal drag:

$$\frac{\partial}{\partial \widehat{Y}} \left( \frac{1}{2^{1/n}} \left| \frac{\partial \widehat{U}^{(0)}}{\partial \widehat{Y}} \right|^{(1-n)/n} \frac{\partial \widehat{U}^{(0)}}{\partial \widehat{Y}} \right) - 1 = 0$$

223 for the region  $\widehat{Y}_0 < \widehat{Y} < 0$  where  $\widehat{U}^{(0)} > 0$  (this can be shown by vertical integration of (S31a), bearing  
 224 in mind that  $\widehat{\mu} \partial \widehat{U} / \partial \widehat{Z} = 0$  at the ice stream surface at  $\widehat{Z} = 1$ , (27)). On the ice stream side  $\widehat{Y} > 0$ ,  
 225 we have no basal drag and so the equivalent model is

$$\frac{\partial}{\partial \widehat{Y}} \left( \frac{1}{2^{1/n}} \left| \frac{\partial \widehat{U}^{(0)}}{\partial \widehat{Y}} \right|^{(1-n)/n} \frac{\partial \widehat{U}^{(0)}}{\partial \widehat{Y}} \right) = 0.$$

226 The original matching conditions with the ice stream as  $Y \rightarrow \infty$  (25)<sub>1</sub> can then simply be reduced to  
 227 a stress condition at  $\widehat{Y} = 0$ ,

$$\frac{1}{2^{1/n}} \left| \frac{\partial \widehat{U}^{(0)}}{\partial \widehat{Y}} \right|^{(1-n)/n} \frac{\partial \widehat{U}^{(0)}}{\partial \widehat{Y}} = 1 \quad \text{at } \widehat{Y} = 0.$$

228 From (S31b) with (S33a)<sub>2</sub>/(S33b)<sub>2</sub>, we can see that the across-stream velocity  $\widehat{V}^{(0)}$  has no vertical  
 229 profile, either. Vertically integrating the mass balance equation (S31d) with (S33a)<sub>3</sub> and (S33b)<sub>3</sub> and  
 230 (27), we can further show  $\partial \widehat{V}^{(0)} / \partial \widehat{Y} = 0$ , or  $\widehat{V}^{(0)} = \text{constant}$ .

231 Matching with the region  $\widehat{Y} < \widehat{Y}_0$ , where there is no sliding, in principle requires a boundary layer  
 232 around  $\widehat{Y} < \widehat{Y}_0$  whose extent is comparable with ice thickness. The appropriate rescaling in that  
 233 boundary layer is

$$\check{Y} = Y - \tau^{-1} \widehat{Y}_0, \quad \check{Z} = Z, \quad \check{U} = \tau^{-1} U, \quad \check{V} = V, \quad \check{W} = W, \quad \check{P} = P. \quad (\text{S34})$$

234 We do not give full detail of that boundary layer; the result of matching with (S31) and the far field  
 235 as  $\check{Y} \rightarrow -\infty$  is simply the intuitive result that

$$\widehat{U}^{(0)} = \frac{\partial \widehat{U}^{(0)}}{\partial \widehat{Y}} = 0, \quad \widehat{V}^{(0)} = \int_0^1 1 - (1 - \widehat{Z})^{n+1} d\widehat{Z} = \frac{n+1}{n+2} \quad \text{at } \widehat{Y} = \widehat{Y}_0,$$

236 and we have a solution for the sliding velocity of the form

$$\widehat{U}^{(0)} = \frac{2(\widehat{Y} - \widehat{Y}_0)^{n+1}}{n+1},$$

237 with

$$\widehat{Y}_0 = -1.$$

238 Putting  $\widehat{T} = \mathcal{T}$ , the corresponding thermal problem in the region with subtemperate slip is then  
 239 at leading order in  $\tau^2$

$$\tau V_m \frac{\partial \widehat{T}}{\partial \widehat{Y}} + \text{Pe} \tau \widehat{V}^{(0)} \frac{\partial \widehat{T}}{\partial \widehat{Y}} - \frac{\partial^2 \widehat{T}}{\partial \widehat{Z}^2} = \frac{\alpha}{2^{1+1/n}} \left| \frac{\partial \widehat{U}}{\partial \widehat{Y}} \right|^{n+1} \quad \text{for } 0 < \widehat{Z} < 1, \quad (\text{S35a})$$

$$\gamma \tau V_m \frac{\partial \widehat{T}}{\partial \widehat{Y}} - \kappa \frac{\partial^2 \widehat{T}}{\partial \widehat{Z}^2} = 0 \quad \text{for } \widehat{Z} < 0 \quad (\text{S35b})$$

240 subject to the jump conditions

$$\left[ \widehat{T} \right]_{-}^{+} = 0, \quad - \left. \frac{\partial \widehat{T}}{\partial \widehat{Z}} \right|^{+} + \kappa \left. \frac{\partial \widehat{T}}{\partial \widehat{Z}} \right|^{-} = \alpha \widehat{U}^{(0)} \quad \text{at } \widehat{Z} = 0, \quad \widehat{Y}_0 < \widehat{Y} < 0. \quad (\text{S35c})$$

241 As before, we assume that  $\alpha \gg 1$  and  $\text{Pe} \gg 1$ . With  $\alpha \gg 1$ , we require a short vertical length  
 242 scale  $\alpha^{-1}$  to be able to conduct heat generated at the bed through frictional sliding into the ice, and  
 243 a commensurately large migration velocity to balance vertical conduction at that scale. If we assume  
 244 that lateral inflow can also contribute to energy balance at the same scale, we require the distinguished  
 245 limit

$$\text{Pe}\tau \sim \alpha^2$$

246 and can rescale as

$$\check{V}_m = \text{Pe}^{-1}V_m, \quad \check{Y} = \hat{Y} - \hat{Y}_0, \quad \check{Z} = \alpha\hat{Z}, \quad \check{T} = \hat{T} \quad (\text{S36})$$

247 leading to the leading order diffusive boundary layer problem

$$\frac{\text{Pe}\tau}{\alpha^2} \left( \hat{V}^{(0)} + \check{V}_m \right) \frac{\partial \check{T}}{\partial \check{Y}} - \frac{\partial^2 \check{T}}{\partial \check{Z}^2} = 0 \quad \text{for } 0 < \hat{Z} < 1, \quad (\text{S37a})$$

$$\gamma \frac{\text{Pe}\tau}{\alpha^2} \check{V}_m \frac{\partial \check{T}}{\partial \check{Y}} - \kappa \frac{\partial^2 \check{T}}{\partial \check{Z}^2} = 0 \quad \text{for } \hat{Z} < 0, \quad (\text{S37b})$$

248 subject to the jump conditions

$$\left[ \check{T} \right]_{-}^{+} = 0, \quad - \left. \frac{\partial \check{T}}{\partial \check{Z}} \right|_{-}^{+} + \kappa \left. \frac{\partial \check{T}}{\partial \check{Z}} \right|_{-}^{-} = \hat{U}^{(0)} = \frac{2\check{Y}^{n+1}}{n+1} \quad \text{at } \check{Z} = 0. \quad (\text{S37c})$$

249 The outer problem in  $\check{Z} = \alpha\hat{Z}$  to this advection-diffusion boundary layer problem is simply the leading  
 250 order (in  $\alpha^2 \sim \text{Pe}\tau$ ) version of (S35), which is the pure advection problem

$$\frac{\text{Pe}\tau}{\alpha^2} \left( \hat{V}^{(0)} + \check{V}_m \right) \frac{\partial \check{T}}{\partial \check{Y}} = 0 \quad \text{for } 0 < \hat{Z} < 1, \quad (\text{S38a})$$

$$\gamma \frac{\text{Pe}\tau}{\alpha^2} \check{V}_m \frac{\partial \check{T}}{\partial \check{Y}} = 0 \quad \text{for } \hat{Z} < 0, \quad (\text{S38b})$$

251 leading to the conclusion that, outside the diffusive boundary layer with height above or below the  
 252 bed described by  $\check{Z} \sim O(1)$ , we simply have the far-field temperature field advected from  $\check{Y} = 0$ .

253 From the rescaling above, we can immediately see that we expect

$$V_m = \text{Pe}\check{V}_m = \frac{\alpha^2}{\tau} f \left( \frac{\text{Pe}\tau}{\alpha^2}, \gamma, \kappa \right)$$

254 for some function  $f$  (in fact, the dependence on  $\kappa$  and  $\gamma$  can be shown to collapse onto a dependence  
 255 on the product  $\kappa\gamma$  alone). It turns out we can compute the function  $f$  exactly, which we do below.

256 The boundary conditions (S37c) only hold up to  $\check{Y} = -\hat{Y}_0 = 1$ . However, in the diffusion problem  
 257 (S37),  $\check{Y}$  is the time-like variable ( $\check{Z}$  being space-like), and if we are only interested in the solution  
 258 for  $0 < \check{Y} < -\hat{Y}_0$  (the region where subtemperate slip is possible), we can without loss of generality  
 259 treat (S37) as applying for all  $\check{Y} > 0$ , which permits the problem to be solved by Laplace transforms.  
 260 Define

$$\tilde{f}(s) = \mathcal{L}(f)(s) = \int_0^\infty f(\check{Y}) \exp(-s\check{Y}) \, d\check{Y}.$$

261 Then

$$\mathcal{L}(\check{Y}^{n+1}) = s^{-(n+2)}\Gamma(n+2)$$

262 where  $\Gamma$  is the standard gamma function. Let

$$\check{T} = \nu - 1 + \Theta,$$

263 so that (34c) becomes  $\Theta = 0$  at  $\check{Y} = 0$ . Transforming (S37) gives

$$sv^\pm \tilde{\Theta} - \frac{\partial^2 \tilde{\Theta}}{\partial \check{Z}^2} = 0$$

264 with  $v^+ = \text{Pe}\tau(\check{V}^{(0)} + \check{V}_m)/\alpha^2$  for  $\check{Z} > 0$ ,  $v^- = \gamma\text{Pe}\tau\check{V}_m/(\alpha^2\kappa)$  for  $\check{Z} < 0$ , and

$$\left[\tilde{\Theta}\right]_{-}^{+} = 0, \quad -\left.\frac{\partial\tilde{\Theta}}{\partial\check{Z}}\right|_{-}^{+} - \kappa\left.\frac{\partial\tilde{\Theta}}{\partial\check{Z}}\right|_{-}^{-} = \frac{2s^{-(n+2)}\Gamma(n+2)}{n+1} \quad \text{at } \check{Z} = 0.$$

265 Matching the outer problem additionally requires  $\tilde{\Theta} \rightarrow 0$  as  $\check{Z} \rightarrow \pm\infty$ . This has solution

$$\tilde{\Theta} = A \exp\left(\mp\sqrt{sv^{\pm}}\check{Z}\right),$$

266 the upper sign being chosen consistently for  $\check{Z} > 0$ , the lower for  $\check{Z} < 0$ . The flux condition at  $\check{Z} = 0$   
267 requires that

$$A\left(\sqrt{v^+s} + \kappa\sqrt{v^-s}\right) = \frac{2s^{-(n+2)}\Gamma(n+2)}{n+1}.$$

268 so that the Laplace transform of  $\Theta$  at the bed is given by

$$\tilde{\Theta}\Big|_{\check{Z}=0} = A = \frac{2s^{-(n+5/2)}\Gamma(n+2)}{(n+1)\left(\sqrt{v^+} + \kappa\sqrt{v^-}\right)}.$$

269 We can now take the inverse Laplace transform; by inspection,

$$\Theta(\check{Y}, 0) = \frac{2\Gamma(n+2)}{(n+1)\Gamma(n+5/2)\left(\sqrt{v^+} + \kappa\sqrt{v^-}\right)}\check{Y}^{n+3/2}.$$

270 At  $\check{Y} = -\hat{Y}_0 = 1$ , we must have temperature reaching the melting point  $\check{T} = 0$ , which becomes  
271  $\Theta = 1 - \nu$ , so the migration velocity is determined by

$$\frac{2\Gamma(n+2)}{(n+1)\Gamma(n+5/2)\left(\sqrt{v^+} + \kappa\sqrt{v^-}\right)} = 1 - \nu,$$

272 or, using the definition of  $v^{\pm}$ ,

$$\frac{2\Gamma(n+2)}{(n+1)\Gamma(n+5/2)}\frac{\alpha}{(1-\nu)\sqrt{\text{Pe}\tau}} = \sqrt{\hat{V}^{(0)} + \check{V}_m} + \sqrt{\kappa\gamma\check{V}_m}.$$

273 This is solvable in closed form; here we give only the (relatively simpler) solution for  $\kappa\gamma = 1$ , the case  
274 also considered in the main paper. Then, also recalling that  $\check{V}_m = \text{Pe}^{-1}V_m$  and  $\hat{V}^{(0)} = (n+1)/(n+2)$ ,  
275 we can find the original migration velocity  $V_m$  as

$$V_m = \frac{\alpha^2}{\tau} \left[ \frac{1}{n+1} \frac{\Gamma(n+2)}{\Gamma(n+\frac{5}{2})} - \frac{(n+1)^2}{4(n+2)} \frac{\Gamma(n+\frac{5}{2})}{\Gamma(n+2)} \frac{\text{Pe}\tau}{\alpha^2} \right]^2. \quad (\text{S39})$$

276 This formula is valid when the term in square brackets is non-negative (the term in square bracket  
277 being negative corresponds to insufficient heat production or too-rapid advection to cause widening  
278 of the ice stream).

## 279 References

- 280 Barcion, V. and MacAyeal, D. R. (1993). Steady flow of a viscous ice stream across a no-slip/free-slip  
281 transition at the bed. *Journal of Glaciology*, 39:167–185.
- 282 England, A. (1971). *Complex Variable Methods in Elasticity*. J. Wiley & Sons, Ltd., London.
- 283 Haseloff, M. (2015). *Modelling the migration of ice stream margins*. PhD thesis, The University of  
284 British Columbia, Retrieved from <http://hdl.handle.net/2429/54268>.

- 285 Haseloff, M., Schoof, C., and Gagliardini, O. (2015). A boundary layer model for ice stream margins.  
286 *Journal of Fluid Mechanics*, 781:353–387.
- 287 Holmes, M. H. (2013). *Introduction to Perturbation Methods*. Springer New York.
- 288 Muskhelishvili, N. I. (1992). *Singular integral equations*. New York: Dover Publications, Inc.  
289 unabridged republication of 2nd edition published by P. Noordhoff, Groningen, 1953.
- 290 Rice, J. (1967). Stresses due to a sharp notch in a work-hardening elastic-plastic material loaded by  
291 longitudinal shear. *Journal of Applied Mechanics*, 34(2):287–298.
- 292 Rice, J. R. (1968). A path independent integral and the approximate analysis of strain concentration  
293 by notches and cracks. *Journal of Applied Mechanics*, 35(2):379–386.
- 294 Schoof, C. (2004). On the mechanics of ice-stream shear margins. *Journal of Glaciology*, 50:208–218.
- 295 Schoof, C. (2012). Thermally driven migration of ice-stream shear margins. *Journal of Fluid Mechan-*  
296 *ics*, 712:552–578.
- 297 Suckale, J., Platt, J. D., Perol, T., and Rice, J. R. (2014). Deformation-induced melting in the margins  
298 of the West Antarctic ice streams. *Journal of Geophysical Research*, 119:1004–1025.